

Frequency Coverage of the ATA Front-end

David R. DeBoer¹, William J. Welch², Matt Fleming², John Lugten², Greg Engargiola², Doug Thornton², Seth Weiman³, Sandy Weinreb⁴, Niklas Wadefalk⁴, Charlie Cox⁵, Ed Ackerman⁵, Douglas Bock², Geoff Bower²

¹SETI Institute, ²University of California at Berkeley, ³Minex Engineering, ⁴California Institute of Technology, ⁵Photonic Systems

Abstract

This memo describes the Allen Telescope Array front-end and some of the radio frequency tests and modeling that quantify and aid in understanding its performance. A passive feed electromagnetically identical to the active feed was constructed in order to measure some intrinsic feed properties such as the input reflection coefficient and the transmission coefficient relative to various standard antennas. The feed was found to operate over the band from 500 MHz to 14.5 GHz, somewhat wider than the original specification of 0.5 GHz -12 GHz. High spectral resolution transmission tests show there are very few resonant drop-outs either in the antenna itself or in the dewar cavity where the transmission lines to the LNA are located. One small resonance was found in one of the two polarizations at 9.3 GHz. The active cryogenic feed will be installed and tested. The measured spectral responses of the other front-end components are also shown.

1. Introduction

The Allen Telescope Array has an unprecedented amount of flexibility in observing modes, which is predicated on two basic and unique aspects of the design¹: (1) the use of many relatively small dishes and (2) the delivery of nearly 11 GHz of bandwidth from each antenna to the central processing building. These two points are interrelated, in that with many dishes one must minimize the cost of the electronics at each antenna and bringing back the entire desired bandwidth is the cheaper option. It also turns out to be much better – however, before this project the means to do so either didn't exist, were inadequate or too expensive.

The Allen Telescope Array has solved these dilemmas by designing a unique ultra-broadband feed with inexpensive cryogenically cooled MMIC low-noise amplifiers very near the terminals, and developing inexpensive analog fiber-optic transmitters. This memo describes these features and provides some early performance measurements demonstrating the requisite frequency coverage of the front-end.

¹ “Moore’s Law” electronics also enable this flexibility, but that harvest is reaped by all.

II. Description of The ATA Front-End

Figure II.a shows the ATA front-end (an early version, since other incorporated antenna components now preclude a good front-end picture). It consists of two items: (1) the feed and (2) the post-amplifier/transmitter sub-system (PAX). The feed consists of the “jagged” log-periodic arms with an interior solid metal pyramidal structure that houses the low-noise amplifier (LNA) and cryogenics. The PAX houses the variable gain post-amplifier module (PAM) and the optical transmitter (OTX). The fiber-optic cable (yellow cord dangling down) goes directly back to the processor building. Figure II.b shows a cut-away drawing of the feed with the interior electronics and Figure II.c shows the interior of the PAX.

The radio frequency (rf) signals are received by the feed and fed to the cryogenic low-noise amplifiers near the tip of the feed. Coaxial cables bring them back to the PAX, inside of which is the PAM, which amplifies them for transmission to the processor building via the analog fiber-optic link. The OTX is the device within the PAX that converts the rf signal to an optical signal and transmits them back to the processor building.

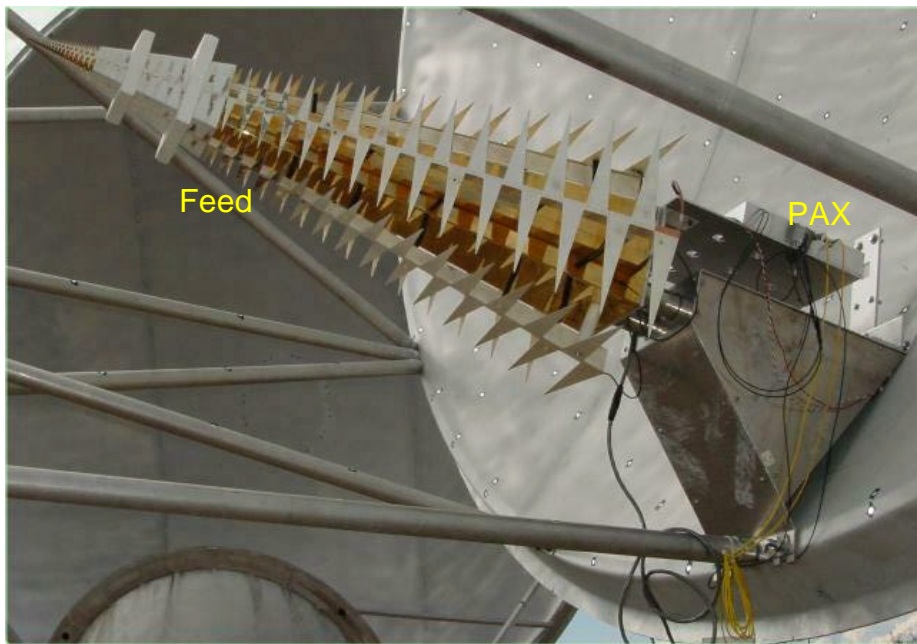


Figure II.a: The Allen Telescope Array front-end, consisting of the feed and the PAX. The mount allows it to be remotely adjusted for focusing.

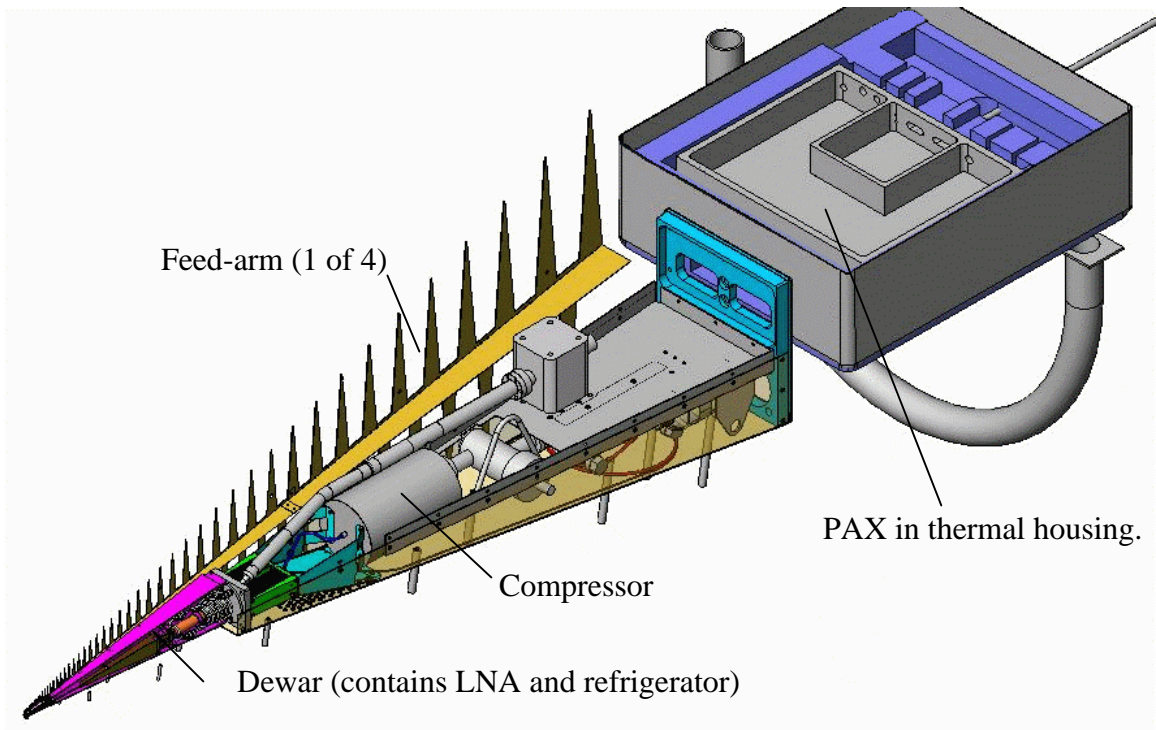


Figure II.b: Cut-away view of the front-end. Only one of the four feed-arms are shown, as well as only half of the pyramid cover, dewar and PAX thermal housing.

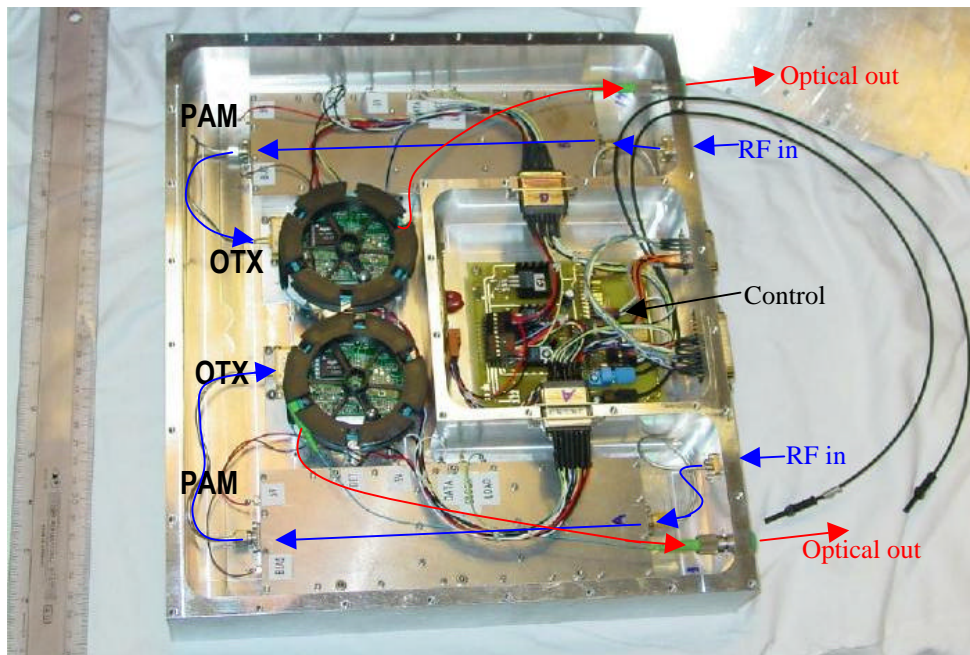


Figure II.c: Picture of the interior of a PAX. The two PAM's and OTX's are marked, and the controller/power is to the middle-right. The blue arrows show the microwave signal paths in and the red arrows follow the optical path out. The black cables are optical control cables, communicating to the element controller in the alidade.

III. Passive Feed Tests

A version of the final feed has been constructed which is complete in all the electromagnetic details but without having the LNA installed. Thus, it contains the dewar, the feed tip circuit, the glass window to the dewar with its matching circuit, the transmission lines to the passive balun, and the balun up to the location of the LNA. In place of the LNA, a coaxial cable six feet in length connects to the outside of the pyramid. Both polarizations are brought out. This passive version allows the reflection and transmission coefficients to be directly measured with an HP 8722ES network analyzer. The balun is a slight variant of the balun to be used with the amplifier in order to match the 50Ω cable. The actual balun matches to 100Ω .

A dual polarization LP antenna may be regarded as a matched directional coupler where the E- and H-plane active regions, which absorb orthogonally polarized free space modes, correspond to the thru and coupled ports. The balanced terminal pairs correspond to the input and isolated ports. The terminals are then cascaded with another four-port device that is the balun/twin-lead from the terminals to the accessible coaxial ports (see Figure III.a). Shown are some primary paths when exciting port 1. Absorber tiles were placed around the antenna during these measurements, so ports 2' and 3' were generally matched. For illustrative purposes, a few short-cuts are taken from strict circuit theory in the ensuing discussion.

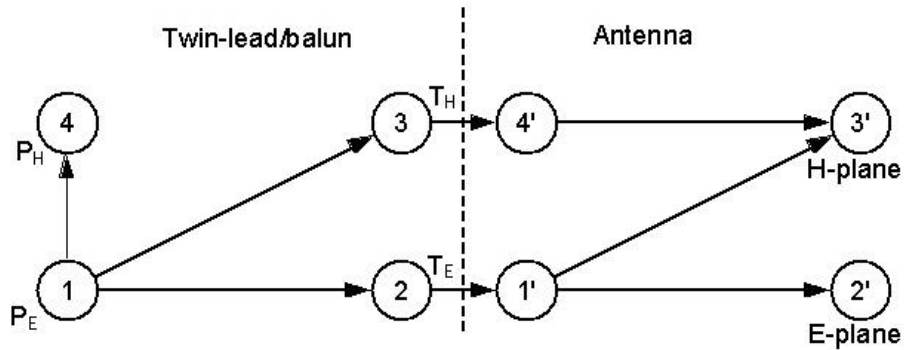


Figure III.a: Scattering diagram of the cascaded antenna and twin-lead/balun. P are the physical ports (the coaxial connectors), T are the antenna feed terminals, and E-plane/H-plane are the radiated dual-linear polarizations.

A. Transmission from the Antenna to Various Test Antennas

Figure III.b shows the transmission using a small spiral antenna that nominally operates over 2 GHz - 18 GHz (nominally $S_{12'}$ in Figure III.a). The figure shows that the feed and balun operate up to 14.5 GHz, significantly beyond the specification of 12 GHz. This is not surprising since neither the feed nor balun are resonant devices. In addition to this wideband scan, the spiral has been used at higher spectral resolution for a search for transmission resonances. Figure III.c is an example of one of the scans that covers 1 - 4 GHz with 801 points, giving a resolution of about 3 MHz. Evidently there are no sharp resonant dropouts associated with either the feed or the dewar structure in this scan. In one polarization there are no dropouts in any part of the spectrum. In the other

polarization there is one sharp but shallow resonance at 9.3 GHz. There is also a broad minimum of about 3 dB depth at 5.3 GHz in both polarizations which is discussed below.

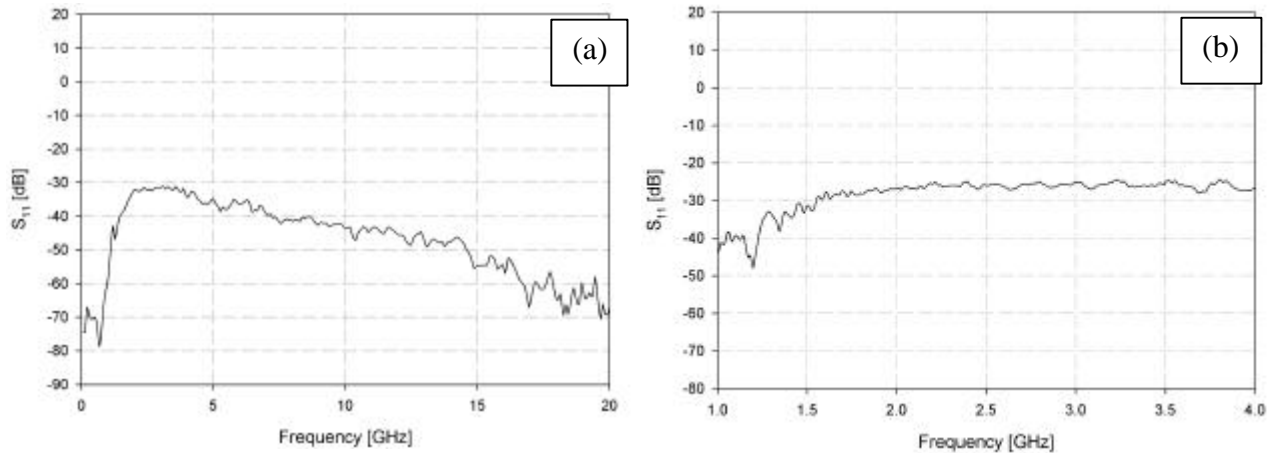


Figure III.b: A scan of the transmission between the ATA feed and a small equiangular spiral antenna that operates over 2 - 18 GHz. The ATA feed and balun evidently work all the way to about 14.5 GHz. This is just one polarization, and the other polarization looks essentially the same.(b) A high resolution scan of the transmission between the ATA feed and the spiral antenna: 1 - 4GHz with 801 spectral points. The spectral resolution is about 3 MHz, and no sharp resonant drop-outs are observed. Thus, neither the antenna nor the region of transmission through the dewar show any resonant transmission nulls.

B. Isolation of the Two Polarizations Ports

Measuring the desired cross polarization coupling ($S_{13'}$ in Figure III.a) would require injecting E-polarized radiation into the antenna (exciting port 3') and measuring the signal at the "coupled" terminal pair (1). The practical lab measurement however, is S_{41} , the "isolation", which is an unknown function of $S_{13'}$. S_{41} is the amount of power reflected back in the opposite polarization and is indicative of the amount of "cross-talk" between the polarizations between the balun and the active region of the feed. S_{41} and S_{11} quantify the amount of power not transmitted (or received) by the feed and hence both impact the aperture efficiency. A small value for S_{41} is a necessary, but not sufficient condition for good cross-polarization performance and this antenna shows a maximum value of about -30 dB. This strengthens the case for good *broad-band* performance, since measurements at L-band show cross-polarization on the antenna to be better than -23 dB. Any resonances would likely show up in this measurement of isolation.

C. Input Impedance Measurements of the Feed

With a frequency scan over 0.05 to 12 GHz converted to a time delay echo measurement using the Fourier transform option, it is possible to measure separately the reflection coefficients of the separate components along the line and at the feed (S_{11} and $S_{1'1'}$ with varying terminals). The delay to the feed tip was measured by placing a razor blade across the feed tip and noting the spike in the scan. Introducing a time gate after the

feed-tip and then turning off the transform shows the reflection coefficient of the antenna alone. This is shown in Figure 3 and is corrected for the losses in the input cable, which were measured separately. The average level is -20.2, corresponding to a VSWR of 1.2, showing that the antenna is an excellent match except for the region around 5.3 GHz. This region corresponds to a place on the feed where the feed standoffs closest to the tip are located. Both polarizations show the same effect, and it can be identified by placing one's fingers on the feed at the standoffs. The simplest cure for this problem is to leave these standoffs off. Another possibility would be to try to find thinner standoffs. Either way the effect can be reduced or eliminated.

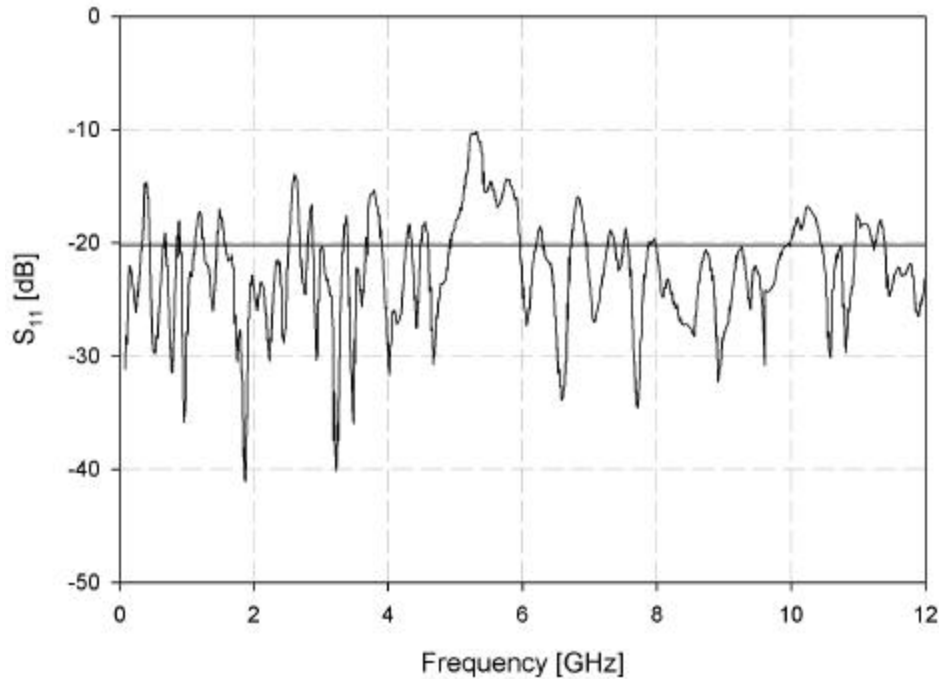


Figure III.c: Spectrum of S_{11} with a time gate placed just past the tip circuit board. This shows the input match of the antenna only. The average level of reflection corresponds to a VSWR of 1.2. The maximum VSWR (excluding the region at 5.3 GHz) is about 1.3. The excess reflection at 5.3 GHz is due to the first set of standoffs on the antenna.

Figure III.d is a drawing of the region interior to the pyramid where the dewar is located. The dewar glass seal is located at 1.692 inches from the tip. In front of it at 1.129 and 1.419 inches are two teflon disks which improve the electrical match of the glass seal. The tip of the radiation shield is at 3.166 inches, and the transition between the transmission lines and the tip of the baluns is at 3.707 inches. The baluns end at 8.593 inches. Setting a gate at the end of the balun and then turning off the transform shows the spectrum of the reflection coefficient, S_{11} , as it will be seen by the LNA when it is in place. Figure III.e shows the spectrum of the reflection, at a maximum of about -10dB, which is a satisfactory input termination for the LNA, although we expect to lower it to perhaps -13dB. It appears to be due largely to the transition between the input two wire transmission line and the tip of the balun, probably associated with the discontinuity between the glass balun and air.

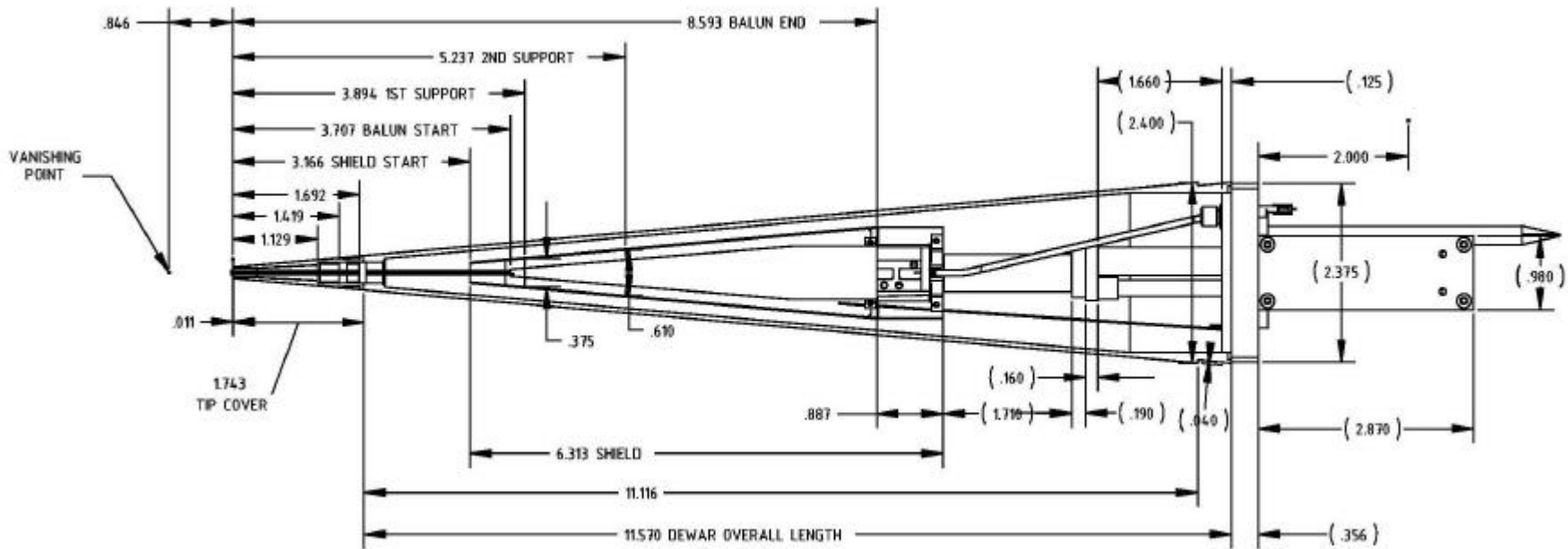


Figure III.d: A drawing of the region interior to the pyramid containing the dewar. The tip circuit board is located at the left end. The time gate for Figure III.e is set just outside the tip circuit board. The dewar glass seal is 1.692" from the tip board. The two matching teflon pieces are at 1.129" and 1.419". The transition from the parallel transmission line wires to the balun is at 3.707". The end of the balun where the LNA will be mounted is at 8.593". For the present tests, a coaxial cable is attached at the end of the balun in place of the LNA. For the spectrum of Figure III.e, the time gate is set at the balun end point to show the match seen by the LNA.

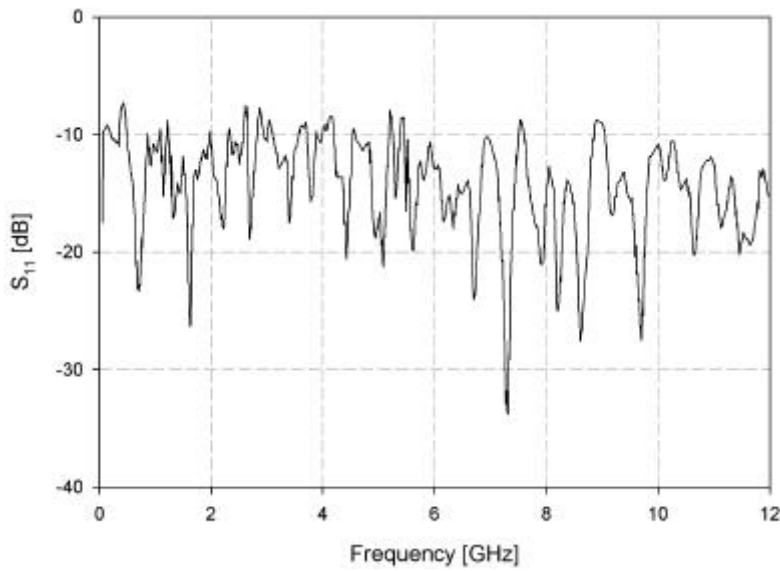


Figure III.e: Spectrum of S_{11} with a time gate set for the location of the LNA to show the match faced by the LNA, corrected for cable loss. The match is thus -10db or better as seen by the LNA.

IV. Measured and Modeled Component Performance

A. Feed and Optics

As described in the previous section, a passive feed has been constructed to measure the intrinsic frequency performance, which is seen to be quite good. Patterns on the antenna will be shown in the subsequent memo. Figure IV.a shows the computed gain and SWR of the feed (solid line) and the expected performance of a feed extended by about 28" to better enable performance at 327 MHz (dashed line). These calculations show the ATA feed working well to about 475 MHz, and the extended feed working well to about 285 MHz. The feed and its internal connections is expected to contribute about 15-20 K of noise across the band (see ATA Memo #6).

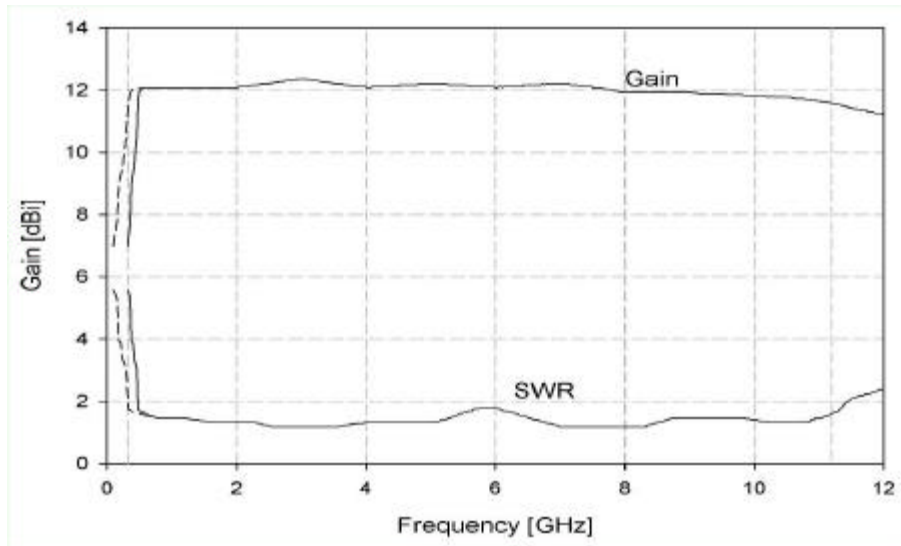


Figure IV.a: Calculated feed gain and standing wave ratio (SWR) for the ATA feed as built (solid line). The dashed line shows the extended performance for temporary feed extensions of 28". The light gray vertical dashed lines mark 327 MHz and 11.2 GHz.

Previous ATA Memos (#16, #25, #29, #49) discuss the optical performance of the feed/antenna system. The nominal in-focus efficiency is about 62%. Since the phase center of the feed moves with frequency, it is desirable to have a means of focusing the feed (a mid-band fixed focus decreases the aperture efficiency by about 0.75 dB at the band edges). The ATA has such an actuator that is under computer control to focus the antenna as desired.

B. LNA

With the input reflection coefficient of the antenna system as it will be seen by the LNA known, it is possible to calculate the expected noise temperature of the LNA for an operating physical temperature of 77 K. Wadefalk (private communication) has measured the LNA noise parameters at 77 K and has modeled its noise temperature for a 100 Ω line impedance and the worst-case reflection from Figure III.e. The figure shows only the magnitude of the reflection as a function of frequency, and Wadefalk assumed a constant reflection of -10 dB across the band (worst case) taking its location to be at the tip of the balun as discussed above. Figure IV.b shows Wadefalk's calculation of the expected spectra of both the noise temperature and the gain of the amplifier. The noise temperature is excellent over the range 0.5 - 12 GHz and, along with the gain, extends well to 15 GHz, as does the operation of the feed as shown in Figures III.b and III.c.

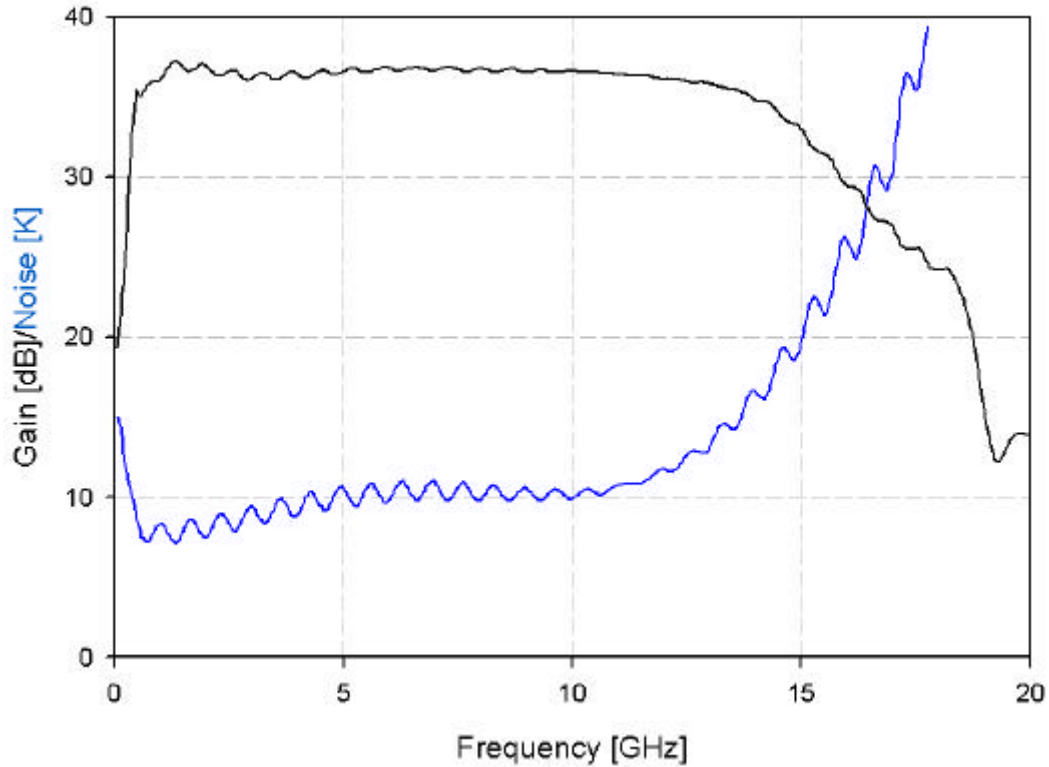


Figure IV.b: Calculated receiver noise and gain for the WBA13 LNA by Wadefalk, based on the measured noise properties of the LNA and the measured reflection coefficient for the feed.

C. Post-Amplifier/Optical Transmitter Subsystem (PAX)

The PAX (shown in Figure II.c) utilizes commodity wide-band electronics in custom designs to provide the variable gain and fiber-optic link. The gain profile is designed such that the post-amplifier and very high input noise figure fiber-optic link (>40 dB) contributes approximately 0.5 K across the band. Figure IV.c shows the measured PAX gain (including the fiber-optic link) cascaded with the amplifier (data shown above) and the stainless-steel coaxial cable in the dewar (18") and the coaxial cable connecting the dewar to the PAX (approximately 5').

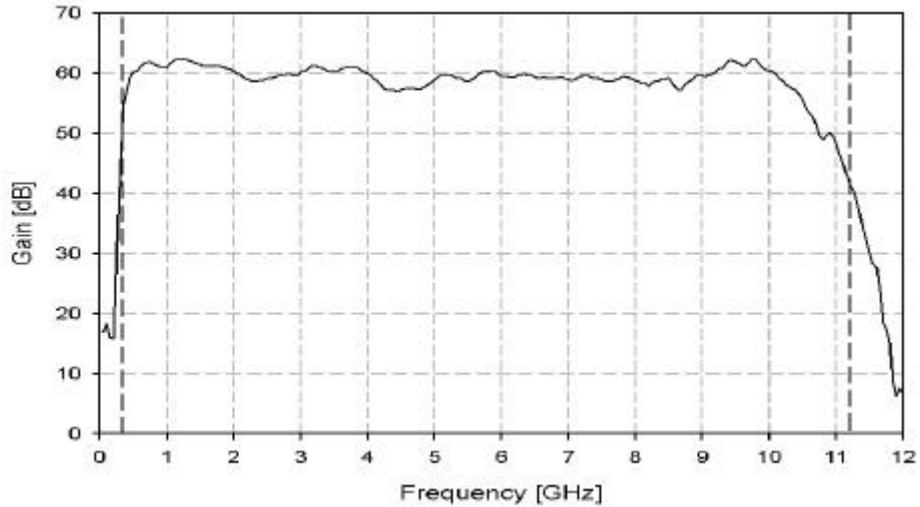


Figure IV.c: Measured performance of the PAX including the entire fiber link, cascaded with the LNA results of Figure IV.b and the cables connecting the LNA with the PAX. The vertical dashed lines mark 327 MHz and 11.2 GHz.

V. Measured Performance of the Cryogenic Feed

The system temperature is determined by the components discussed in the previous section, as well as the galactic background, the radiative temperature of the atmosphere and the spillover onto the ground. Using the flux from the galactic anti-center (the reason for which is explained in the following section, the choice being irrelevant for frequencies above about 1 GHz) and the modeled atmosphere at Hat Creek assuming a look angle of 45° and 50% relative humidity, Figure V.a shows the expected system temperature and Figure V.b shows the expected A_e/T_{sys} when the system is fully functional and optimized. The dashed line shows the specification for the first unit. This level was chosen since it does require achievement of a quite good cryogenic system, but recognizes that the first front-end may not achieve the eventual performance level. It was also set prior to the recent measurements indicating better than expected performance of the low noise amplifier.

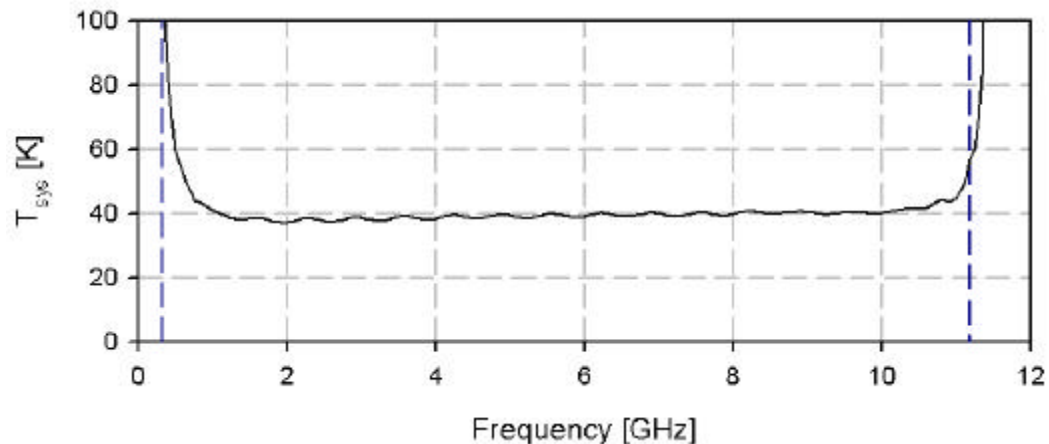


Figure V.a: Computed cascaded system temperature, assuming the Galactic anti-center in the beam, a 50% RH atmosphere, an elevation of 45° and the cascaded system from Figure 8.

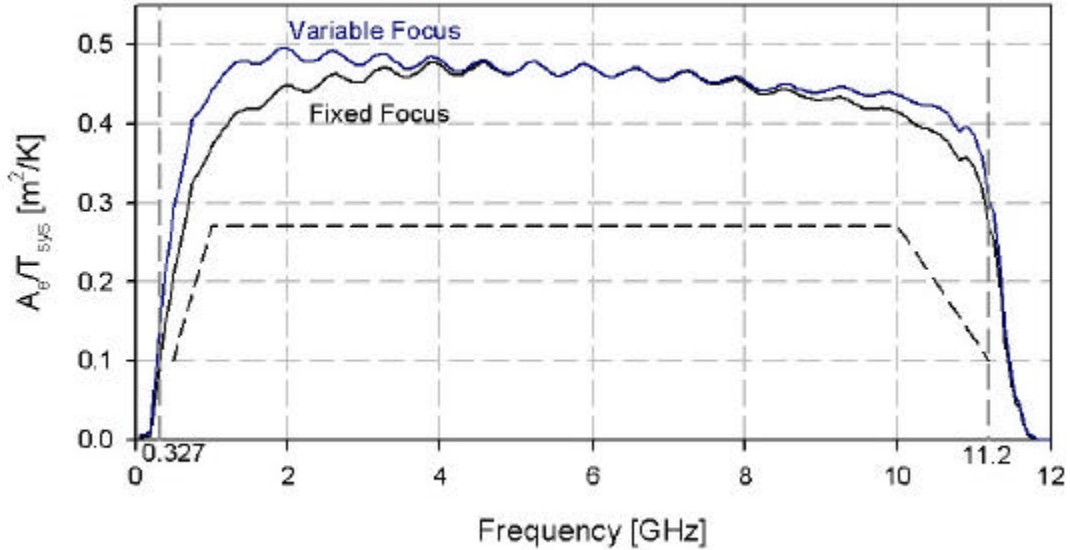


Figure V.b: The corresponding expected sensitivity (m^2/K) assuming a fixed focus at 6.25 GHz (black line) and a variable focus, which extends from 1.2 GHz to 11.2 GHz.

VI. Predicted Performance at 327 MHz

Although not originally designed to operate at 327 MHz, the ATA still has significant performance at that frequency. The feed is the limiting factor but, as shown in a previous section, may be temporarily and easily modified to perform quite well down to about 285 MHz. Alternatively, a more simple UHF feed may be designed and temporarily installed, which may yield even better performance for this experiment. The rest of the components all work down to that frequency, including the quartz balun, where measurements show an acceptable -10dB insertion loss at that frequency. We are therefore confident that the ATA will perform quite well at 327 MHz, with one of the aforementioned feed changes. Figures VI.a and VI.b show the expected performance assuming that an extended ATA feed is utilized, where Figure VI.a shows the expected T_{sys} and Figure VI.b the A_e/T_{sys} . Note that much of the roll-off is unavoidable, due to the increasing background flux of galactic origin. That component is shown as the dashed line in Figure VI.a. (As mentioned, this assumes the flux level of the Galactic anti-center).

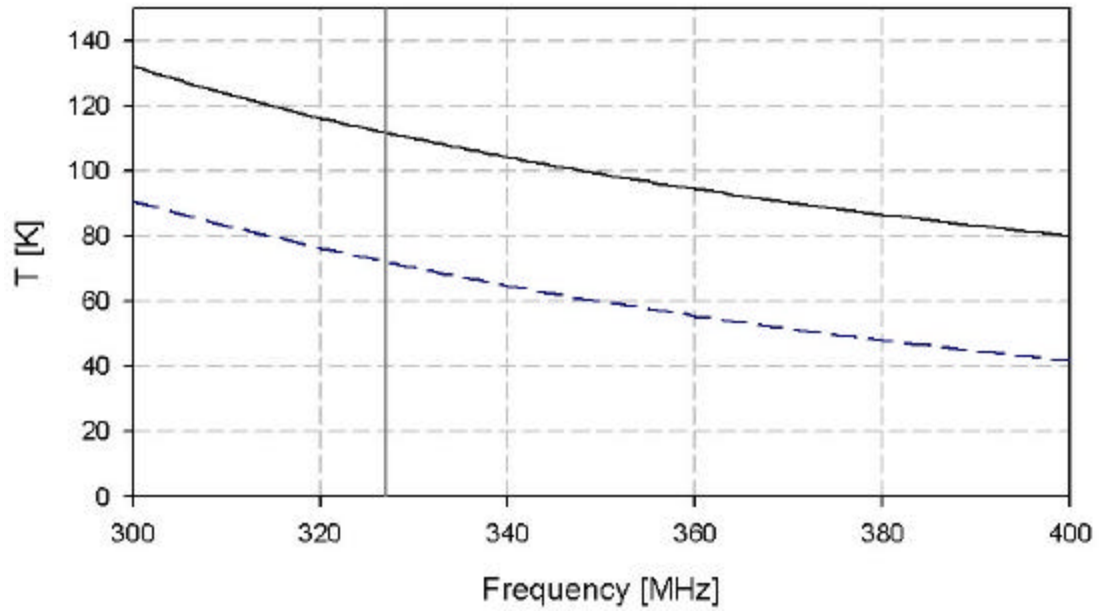


Figure VI.a: Same as Figure V.a, zoomed in to look near 327 MHz. The dashed line shows the contribution of the Galactic anti-center.

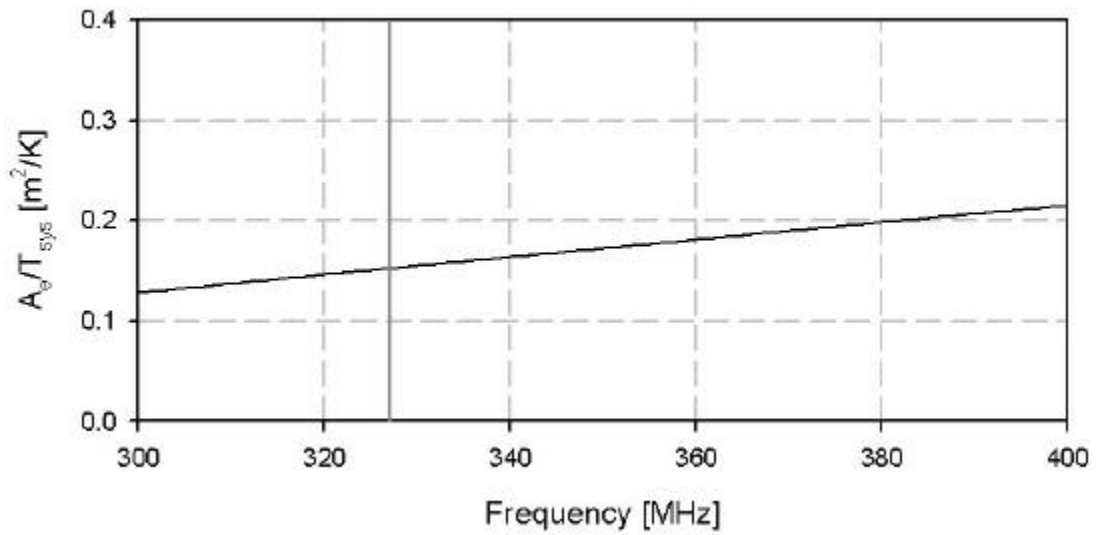


Figure VI.b: Same as Figure V.b, zoomed in to look near 327 MHz.